Cell Cultivation Under Different Gravitational Loads Using a Novel Random Positioning Incubator

Tatiana Benavides Damm,[1,2] Isabelle Walther,[1] Simon L. Wüest,[1,3] Jörg Sekler,[3] Marcel Egli[1]

[1]CC Aerospace Biomedical Science & Technology, Space Biology Group, Lucerne University of Applied Sciences and Arts (HSLU), Hergiswil, Nidwalden, Switzerland

[2]Institute for Biomechanics, Eidgenössische Technische Hochschule Zürich (ETHZ), Zürich, Switzerland

[3]Institute for Automation Engineering, University of Applied Sciences and Arts Northwestern Switzerland (FHNW), Brugg-Windisch, Aargau, Switzerland

ABSTRACT: Important in biotechnology is the establishment of cell culture methods that reflect the in vivo situation accurately. One approach for reaching this goal is through 3D cell cultivation that mimics tissue or organ structures and functions. We present here a newly designed and constructed random positioning incubator (RPI) that enables 3D cell culture in simulated microgravity (0 g). In addition to growing cells in a weightlessness-like environment, our RPI enables long-duration cell cultivation under various gravitational loads, ranging from close to 0 g to almost 1 g. This allows the study of the mechanotransductional process of cells involved in the conversion of physical forces to an appropriate biochemical response. Gravity is a type of physical force with profound developmental implications in cellular systems as it modulates the resulting signaling cascades as a consequence of mechanical loading. The experiments presented here were conducted on mouse skeletal myoblasts and human lymphocytes, two types of cells that have been shown in the past to be particularly sensitive to changes in gravity. Our novel RPI will expand the horizon at which mechanobiological experiments are conducted. The scientific data gathered may not only improve the sustainment of human life in space, but also lead to the design of alternative countermeasures against diseases related to impaired mechanosensation and downstream signaling processes on earth.

Biotechnol. Bioeng. 2014;111: 1180–1190.

Introduction

Recent tissue engineering studies have revealed striking discrepancies between the behavior of cells cultured in 3D and 2D, where 3D cell cultures mimicked intact tissue in terms of viability and gene expression (Baharvand et al., 2006; Sun et al., 2006). Indeed, 3D cell culture is one favorable approach for reducing the gap between artificial cultivation in vitro and the in vivo physiological situation. The benefits of 3D cell cultivation over 2D monolayers are featured due to the increased cell to cell contact, as well as cell to extracellular matrix interaction, and the accumulation of nutrients and growth factors (Saltzman et al., 1992). It has been shown that cell growth in 3D can be achieved through the randomized movement employed by rotating bioreactors which simulate microgravity (Freed and Vunjak-Novakovic, 1995). Furthermore, this platform provides a constant circulation of nutrient medium, removing the higher waste concentrations that are usually found in the microenvironment adjacent to the cell surface (Rivera-Solorio and Kleis, 2006).

The first instruments used to simulate microgravity were clinostats, developed in 1879, a long time before the beginning of space exploration, by Julius von Sachs, a botanist who wanted to investigate gravitropism in plants (van Loon, 2007). The uni-axial clinostat worked by slowly rotating the specimens around a longitudinal horizontal axis. In this way, for example, the growing plant was experiencing a continuously reoriented gravity vector over a long period of time. Later on, fast rotating clinostats were developed and introduced to negate the gravitational force on cells growing in culture media. In order to study such cells, the diameter of the rotating part of the clinostat had to be small to avoid the generation of centrifugal forces, and the rotational speed had

to be much faster (40–100 rpm). In the fast rotating clinostat, research on single mammalian cells and unicellular organisms could be performed since small samples no longer experience the turning of gravity as they are in simulated weightlessness (Block et al., 1986). Limitations of the fast rotating clinostat motivated the development of other instruments that allowed larger samples to be cultivated under simulated microgravity. The rotating wall vessel (RWV) is one example of such a device that provides an environment with low-shear forces, allowing cells to grow even as 3D aggregates (Schwarz et al., 1992). Since the late nineties, a 3D clinostat called a random positioning machine (RPM) has been intensively used for ground-based research. The RPM, originally developed by T. Hoson in Japan, applies the principle of neutralizing gravity by vector averaging (Hoson et al., 1997). Numerous experiments have already proven that this technique generates data that is indeed very similar to the data obtained in space (Herranz et al., 2010; Infanger et al., 2006; Pietsch et al., 2012; Schwarzenberg et al., 1999).

As access to real weightlessness in space is very limited and expensive, scientists have always been interested in having earth-bound tools available to perform pilot studies in simulated microgravity. These instruments are of great importance to test hardware and processes under microgravity approaching conditions and in studying biological systems under these specific settings. The RPM, though not totally equal to real space, is a good tool for preparing space experiments, for testing newly developed instruments, and for studying biological systems of interest under simulated weightlessness, as well as for gathering enough valuable data that can be used for statistical purposes. Nevertheless, one of the major constraints of the RPM so far has been that no simulated partial gravity values could be attained. With the increasing interest of the scientific community to return man to the Moon and to go further in the exploration of Mars, studies performed with these two gravity fields (0.16 g and 0.38 g, respectively) are becoming increasingly valuable. At the present time these types of studies have been performed in head-up tilt studies, in body suspension devices, and for a short duration in parabolic flights (Cavagna et al., 2000; Dalmarco et al., 2006; Pavy-Le Traon et al., 1997). Long-term experiments at a cellular level have not yet been possible except when performed in a centrifuge in real space such as during the IML-2 mission in 1994 with the NIZEMI slow rotating microscope (Friedrich et al., 1996). As well as using partial gravity for space related studies, having various gravitational environments available for conducting research opens new approaches to investigate the mechanobiology of cells ranging from single mammalian cells to microorganisms.

In this paper, we present a newly designed and built RPM equipped with an integrated incubator, thus called random positioning incubator (RPI) that in addition to generating simulated microgravity, offers new features such as partial gravity simulation during an extended period of time. Using this machine, environments from close to 0 to almost 1 g can be generated by several algorithms. A machine of this type increases the variety of experiments which can be tested in general and additionally allows the exploration of effects on biological samples in conditions which are difficult to create, such as the gravity field of the Moon or Mars. The data reported in this study was gathered with mouse skeletal myoblasts (adherent cells) and human lymphocytes (non-adherent cells), in an attempt to better understand how deconditioning the cells through mechanical unloading by reducing gravity affects two major physiological mechanisms: the skeletal muscle and the immune system. These two mammalian cell types have repeatedly demonstrated high sensitivity to simulated microgravity (Benavides Damm et al., 2013b; Chang et al., 2012; Sonnenfeld, 2012). As gravity provides a stimulus for their maintenance, we hypothesized that partial gravity exposure would produce changes in their behavior and sought to investigate whether this response was proportionally linear, nonlinear, or set by a threshold with decreasing gravity levels. The answer to this question is essential, not only for aerospace physiology, but also necessary in order to comprehend the effects of mechanical unloading associated with clinical scenarios on earth, such as aging and illness arising from immobilization and prolonged periods of bed rest.

Materials and Methods

Random Positioning Incubator (RPI)

The RPI equipment consists of two independently rotating gimbal-mounted frames, each axis being motorized by an electrical drive to control random, or other positioning, sequences. Through a dedicated algorithm the samples are constantly reoriented with respect to the earth gravity vector. This allows the distribution of the vector in space, leading over time to an average gravity value smaller than 1 g. A unique feature of our present RPM, the RPI version, is the integration of a miniaturized CO_2 incubator including a 14 L test chamber, mounted at the center of rotation of both frames (Fig. 1). The specially functionalized incubator is supplied with electrical power and CO_2 (and other experimental supplies) throughout the experiment's duration. Important data such as temperature, CO_2 levels, and mean gravity values are monitored automatically. Our present RPI will be described in more details elsewhere (manuscript under review).

Myoblasts

C2C12 mouse skeletal myoblasts were obtained from ATCC (American Type Culture Collection, LGC Standards S.a.r.l., Molsheim Cedex, France) and cultured in a medium consisting of Dulbecco's Modified Eagle Medium (Life Technologies, Lucerne, Switzerland) supplemented with 20% fetal bovine serum (PAA, Basel, Switzerland) and 2 mM L-Glutamine (Life Technologies) in a humidified
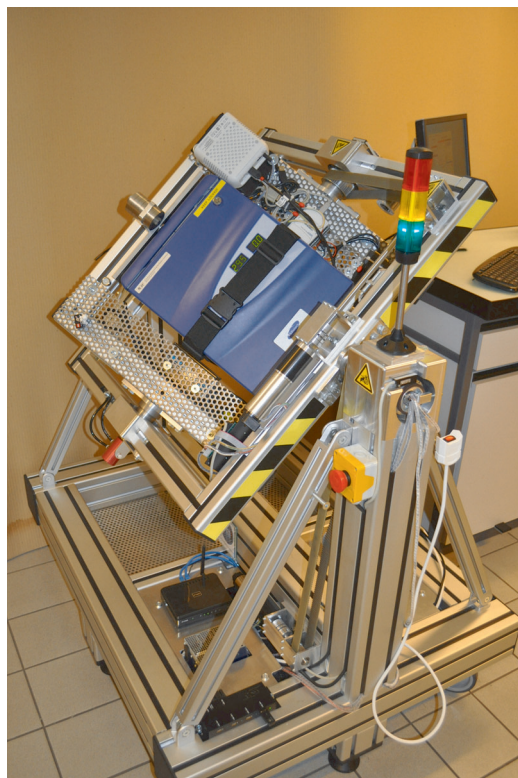
Figure 1. A recent version of the random positioning incubator (RPI) as designed and developed by the project partner FHNW based on collaboration and requirement specifications of ETHZ. The RPI consists of two gimbal-mounted frames, which are driven by electrical motors, and a CO_2 incubator mounted at the center of rotation of both frames.

atmosphere at 37°C in 7% CO_2. Cells were passed every 2 days and were only used for experimentation before the 15th passage. Myoblasts were seeded at 8,000 cells/cm^2 in 25 cm^2 flasks (Semadeni, Ostermundigen, Switzerland) 15 h before the start of each experiment. Immediately before being placed on the RPI, the flasks were carefully filled with media, avoiding the formation of bubbles. Cell counting was performed manually with a hemocytometer (Biosystems, Nunningen, Switzerland) on trypan blue (Life Technologies) treated cells to assess cell concentration and viability, according to the dye exclusion method (Yip and Auersperg, 1972). The counts were carried out in duplicate per independent sample after 24 h of growth on the RPI or inside an incubator under normal culture conditions (1 g control). Cell growth was also monitored with the CellTrace CFSE Cell Proliferation Kit (Life Technologies), according to the manufacturers' protocol. Briefly, cells were stained with 5 μM carboxyfluorescein diacetate, succinimidyl ester (often called CFSE) in phosphate buffered saline + 0.1% bovine serum albumin at 37°C for 10 min. Cells were plated and collected after 24 h of growth under different gravitational conditions, and then re-suspended in 3.7% Cell Fix (BD Biosciences, Allschwil, Switzerland) for overnight storage at 4°C before fluorescence activated cell sorting (FACS) analysis.

CFSE is a dye that passively diffuses into cells, reacting with intracellular amines and forming fluorescent conjugates. Following initial staining of the mother cells, subsequent rounds of cell division dilute the amount of dye inherited by daughter cells by one half with each division. For cell cycle analysis, cells were collected after 10 h of culture on the RPI or on the incubator and fixed. Samples were stored at −20°C in 70% ice cold ethanol for at least 12–18 h prior to staining. Cell cycle was analyzed based on DNA content through propidium iodide (PI) with RNase staining by FACS. CFSE fluorescence intensity and cell cycle profiles were analyzed and quantified with the FlowJo flow cytometry analysis software (TreeStar, Inc., Ashland, OR). To quantify G0/G1, S, and G2/M populations, the Watson model was used to fit the histograms of single gated cells (Watson et al., 1987). FACS Calibur (BD Biosciences) was used for acquisition and appropriate settings for forward and side scatter gates were applied to examine 20,000 events per sample. The blue laser with excitation at 488 nm was used, with FL1 channel detector for CFSE and FL2 channel detector for PI staining. Data (means ± standard deviations) were obtained from three or four independent series of experiments.

Lymphocytes

Whole peripheral blood was obtained from healthy human volunteers. Peripheral blood lymphocytes (PBL) were isolated using Ficoll gradient (Histopaque; Sigma, Buchs, Switzerland), red blood cells were lysed and finally T-cells were purified further using enrichment columns as per the manufacturer's instructions (R&D Systems, Abingdon, United Kingdom). T-cells were re-suspended into RPMI 1640 (Life Technologies) with 10% fetal calf serum (Life Technologies). The cells were loaded at a concentration of 1 to 2 × 10^6 cells/mL inside the "LYCIS" hardware, which has been developed specially for space experiments. This hardware is based on the principle of moving pistons that allows the loading of cells in the absence of air bubbles and the injection of substances rapidly without opening the hardware. The cells were preconditioned at each experimental environment for 60 to 90 min prior to activation with a concanavaline A (conA)/anti CD28 mixture (BD Biosciences) for T-cells or only with conA (Sigma) for the PBL. After 20 to 22 h of incubation at 37°C under the respective gravity conditions, the cells were harvested and stained. The staining was carried out according to the supplier using PE-CD25 marker (Miltenyi Biotec, Bergisch Gladbach, Germany) which is an early marker for lymphocyte activation. Stained cells were analyzed on the FACS Calibur using 10,000 events per sample. The FlowJo software was used to gate the cells and fit the histograms. The 1 g samples of each experiment were considered as 100% activated, and were used to standardize the other samples among the different experiments. A non-activated sample was used as negative control. Data (means ± standard deviations) were obtained from three independent series of experiments.

Algorithms

Simulated microgravity on a RPM is achieved by gravity vector averaging to zero as described earlier (Hoson et al., 1997). Thereby the earth gravity vector is distributed over time by constantly reorienting the samples to random positions, where eventually the mean gravity will converge to a small value. As described below, we adjusted the distribution of the gravity vector in order to obtain a desired mean gravity value. As a quality measure for the distribution of orientation we use the mean gravity over time, defined by

$$G_{\mathrm{mean}} = \sqrt{(G_{X,\mathrm{mean}})^2 + (G_{Y,\mathrm{mean}})^2 + (G_{Z,\mathrm{mean}})^2} \quad (1)$$

Here, the mean gravity values in the three directions are defined as follows:

$$G_{X,\mathrm{mean}} = \frac{\sum_{i=1}^{n} g_{X,i}}{n}, \ G_{Y,\mathrm{mean}} = \frac{\sum_{i=1}^{n} g_{Y,i}}{n}, \ G_{Z,\mathrm{mean}} = \frac{\sum_{i=1}^{n} g_{Z,i}}{n} \quad (2)$$

If the pattern of random positions are chosen such that the earth vector spends more time in one particular area (considered in the local frame of the sample), partial gravity will result. There are numerous motion patterns possible to create simulated partial gravity by fulfilling the above equations. We developed and used three different algorithms; all of them based on a random walk algorithm described elsewhere (manuscript under review). In brief, this random walk algorithm rotates both frames with constant rotational velocity and inverts the direction of rotation (forward or backward) at random times. The velocity transition takes place at a constant rotational acceleration. This unmodified random walk algorithm was employed for the 0 g experiments. The simulated partial gravity level that can be achieved is limited to a certain maximum that depends on the algorithm used and the corresponding parameters. In addition, the accuracy and the time necessary to reach the desired partial gravity value is algorithm-dependent (Fig. 2). The stability of our applied algorithms was verified with numerical simulations (Fig. 3). In this study, we used the following three different algorithms:

Simulated Partial Gravity Based on Random Walk With Two Velocities (Two Velocities)

To achieve a particular mean gravity value, the local vector of one direction is enlarged by making the rotation velocity
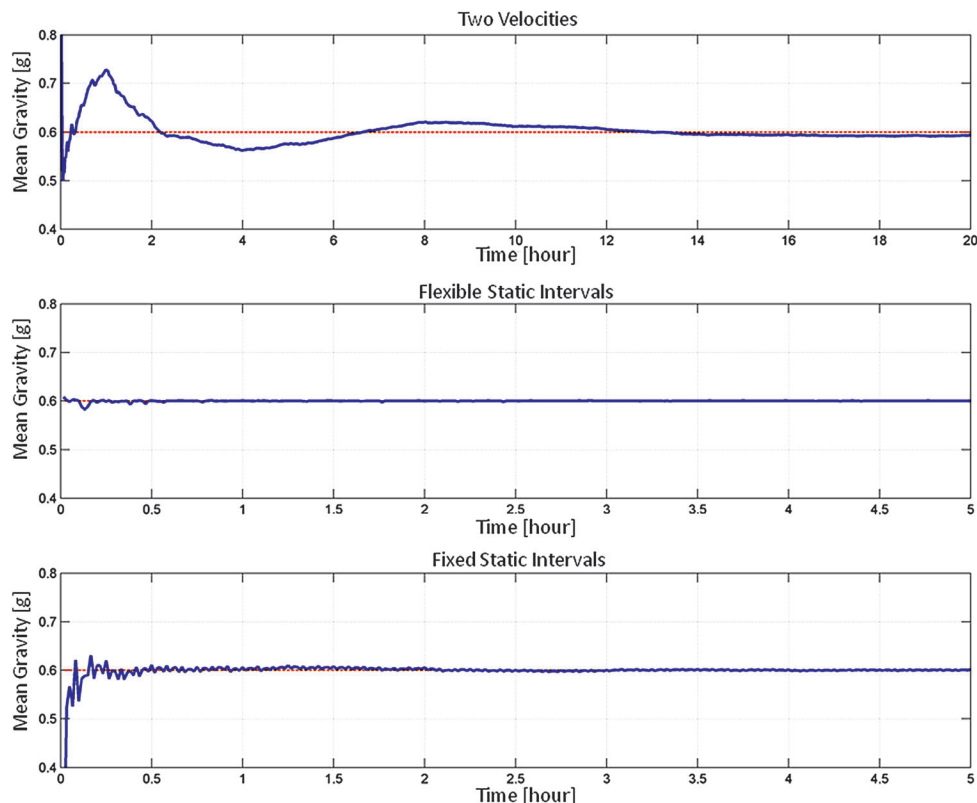

Figure 2. Timeline of the mean gravity values for the algorithms. The Two Velocities algorithm (top track) achieves partial gravity through position dependent rotation velocity, whereby the frames are permanently rotating. The mean gravity value is controlled with a predictive controller. In contrast, the Flexible Static Intervals algorithm (middle track) controls the mean gravity value by particular intervals between random walk and static phases. The interleaving timing of the random walk and static phases is flexible and controlled online. The Fixed Static Intervals algorithm (bottom track) works similarly but has fixed periods of random walk and static phases. The nominal rotational velocity was 60°/s for the three algorithms. Note: for presentation reasons, the time scale is not identical.
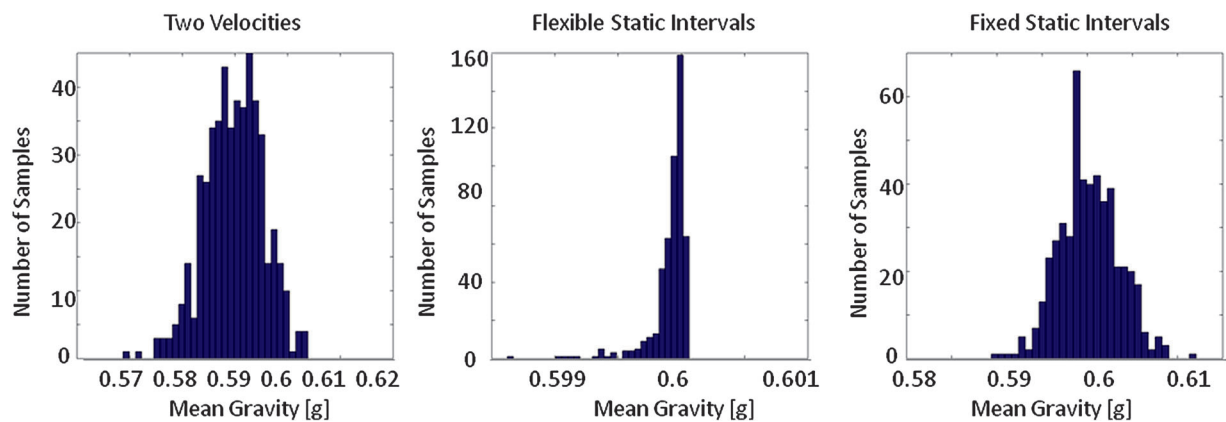
Figure 3. Verification of the stability of the algorithms through numerical simulations; all of the algorithms are based on a random walk pattern which depends on a sequence of random numbers. The stability was verified by 500 numerical runs. The resulting mean gravity value was taken following a simulated experiment of 20 h in the case of Two Velocities algorithm (left), and 5 h in the case of Flexible Static Intervals (middle) and Fixed Static Intervals (right) algorithm. The nominal rotational velocity was 60°/s for the three algorithms.

position dependent. In principle, the RPM slows down, when this vector is pointing downward. Thus, the RPM spends slightly more time in one direction than in the others. The relation of the nominal to the slower velocity determines the resulting mean gravity. Since the random walk algorithm is based on random numbers, two consecutive runs will not reproduce the same result. Therefore, the velocity relation is controlled by a predictive controller: While the nominal (or faster) velocity is fixed, the slower velocity is initially guessed based on numerical simulations. The RPM runs then for 1 h such that the mean gravity value can be stabilized. Based on the deviation from the desired mean gravity, the value of the lower velocity is refined. The RPM subsequently runs again for 1 h, after which the slower velocity is again corrected. This interval of letting the mean gravity stabilize for 1 h with a subsequent refinement of the slower velocity is repeated until the end of the experiment. We were able to achieve up to 0.6 g reliably, which is close to the upper limit. This algorithm ensures that the frames are always in motion. However, it takes at least 2 h to achieve the desired partial gravity value (Fig. 2).

Simulated Partial Gravity Based Random Walk and Flexible Static Intervals (Flexible Static Intervals)

Since random walk reduces the mean gravity value towards zero, this algorithm interleaves the random walk with static phases, whereby the frames are stopped at one particular position. The timing of the static phases is controlled by the computer online, depending on the actual and the desired mean partial gravity value. The algorithm basically stops the RPM at a predefined position if the mean gravity value is smaller than desired and it continuous in random walk if the mean gravity value is larger. In order to suppress too frequent switches between static and random walk, the RPM has to spend a minimum amount of time in random walk until it can switch back again to static mode. This motion pattern allows the simulation of partial gravity values close to 1 g. At

high partial gravity values (>0.6 g) however, one has to keep in mind that the samples would be standing still for most of the time.

Simulated Partial Gravity Based Random Walk and Fixed Static Intervals (Fixed Static Intervals)

This algorithm works like the Flexible Static Intervals algorithm, except that the time spent in random walk or static position is fixed and constant throughout the experiment. The relation of the rotating to the static time determines the resulting mean gravity value. For example, if the frames rotate for 40% of the time in random walk and are static for 60% of the time, a mean gravity of 0.6 g will result. In our experiments we used a cycling period of 2.5 min (e.g., for a 0.6 g experiment the RPM spends 1 min in random walk, followed by 1.5 min standing still, where the cycle is continuously repeated). This algorithm, again, allows reaching partial gravity values close to 1 g. However, the samples would be standing still for most of the time at high partial gravity values (>0.6 g) as is the case when applying the Flexible Static Intervals algorithm.

For all three partial gravity algorithms and the unmodified random walk, the nominal rotational velocity was 60°/s for the myoblast experiments and 40°/s for the lymphocyte experiments.

Results

Cell Proliferation is Decreased in Correlation With Reduced Partial Gravity Levels

One of the most prominent consequences of manned space travel is muscle atrophy (Vandenburgh et al., 1999). It is therefore relevant to examine how muscle maintenance is compromised by prolonged exposure to reduced gravitational forces. C2C12 mouse muscle cells were grown either

under simulated microgravity (0 g), simulated partial gravity (0.2, 0.4, and 0.6 g), or at terrestrial gravity (1 g), and their total numbers were quantified 24 h afterwards. The three different algorithms for partial gravity simulation (see Materials and Methods) were compared to gain insights in their potential to influence the induction of biological effects on the cells. By normalizing cell growth to the 1 g control, an increased proliferation rate is visible as the partial gravity level gets bigger, where the values increased linearly from $43.08 \pm 5.71\%$ at 0 g to 100% at 1 g when using the Two Velocities algorithm (Fig. 4A). Similarly, the Flexible Static Interval algorithms also produced analogous results though with smaller values. However, with the Fixed Static Interval algorithm, the values varied between $52.13 \pm 6.44\%$ at 0.2 g, $48.71 \pm 2.72\%$ at 0.4 g, and $54.70 \pm 5.16\%$ at 0.6 g, thus no relation between the simulated partial gravity level and the cell counts was established. These effects were confirmed by using the alternative analysis method for cell proliferation, CFSE staining, where the median fluorescence intensity (MFI) was determined. The normalized MFI decreased linearly from $269.56 \pm 66.25\%$ at 0 g to 100% at 1 g when using the Two Velocities and Flexible Static Intervals algorithms (Fig. 4B). Thus, cells grown on the RPI at increasing partial gravity levels exhibit a steadily decrease in fluorescence intensity, meaning that the cells divide faster at higher partial gravity levels, accordingly losing fluorescence intensity. However, with the Fixed Static Intervals algorithm, there was no correlation with the partial gravity level of exposure, as the normalized MFI varied between $176.53 \pm 25.19\%$ at 0.2 g, $183.46 \pm 4.58\%$ at 0.4 g, and $161.23 \pm 7.74\%$ at 0.6 g.

Simulated Partial Gravity Does Not Cause an Increase in Cell Death Rate

The possibility of whether the decrease in cell propagation observed in reduced partial gravity levels was due to an increased cell death under these conditions was investigated. After growing myoblasts under simulated partial gravity or at 1 g, no significant difference was observed between all the samples, as they all exhibited nearly 100% viability, irrespective of the type of algorithm used to simulate partial gravity (Fig. 5). In agreement with our previous results, this data indicates that another mechanism such as the cell cycle progression plays a more substantial role in determining the cell growth pace under partial gravity, as the decrease in cell proliferation rate was not due to enhanced cell death in response to gravitational unloading (Benavides Damm et al., 2013b).
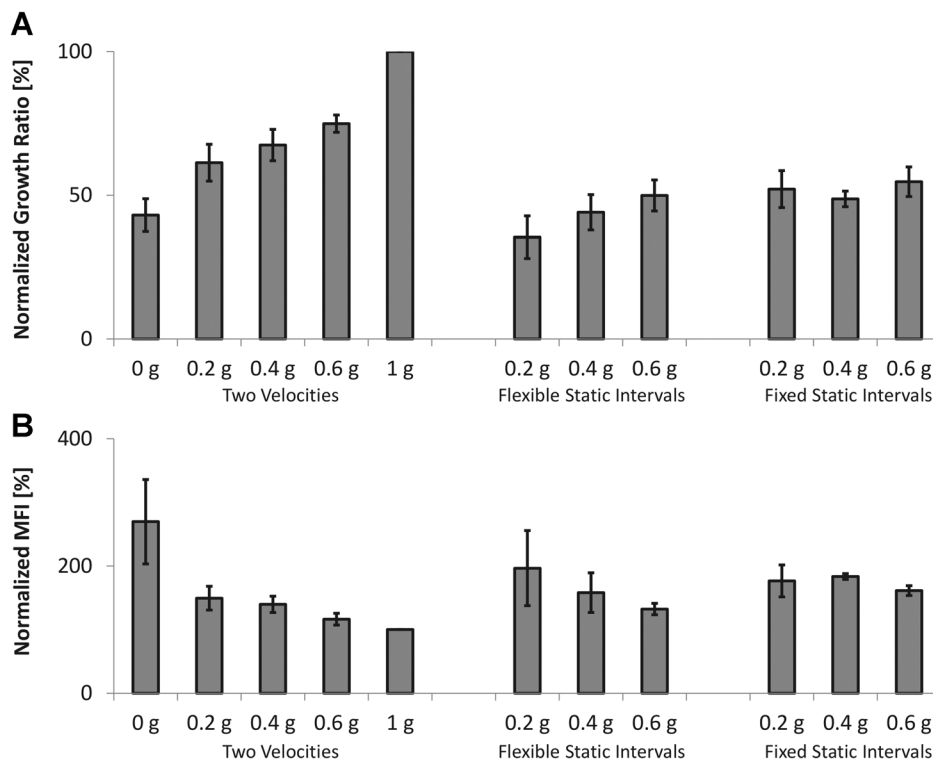

Figure 4. Cell proliferation decreases with reduced partial gravity levels. Cell proliferation was assessed by counting cells manually (**A**) or by CFSE staining (**B**). The counts and median fluorescence intensity (MFI) of cells grown on the RPI after 24 h were normalized to the values of cells grown inside an incubator under normal culture conditions (1 g). Three different algorithms for partial gravity simulation (see Materials and Methods) were compared in the following order: Two Velocities, Flexible Static Intervals, and Fixed Static Intervals. Means ± standard deviations were obtained from three independent series of experiments.
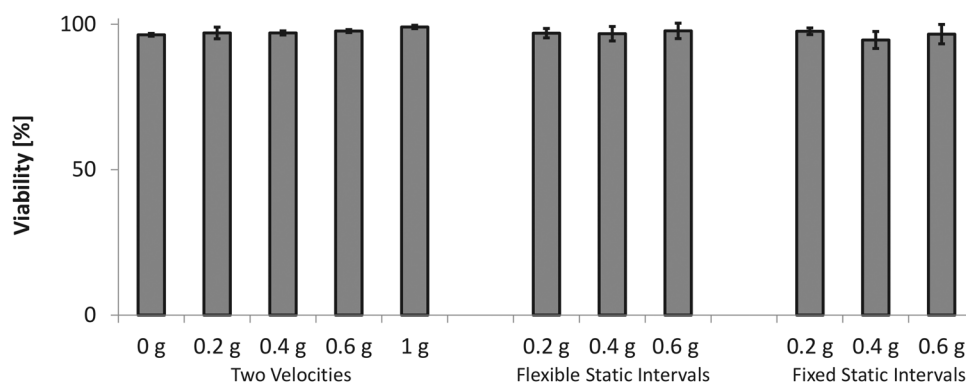
Figure 5. Cell viability is not affected by partial gravity. Cell viability was assessed by counting trypan blue treated cells manually, following 24 h of growth on the RPI or inside an incubator under normal culture conditions (1 g). The three different algorithms for partial gravity simulation (see Materials and Methods) were compared in the following order: Two Velocities, Flexible Static Intervals, and Fixed Static Intervals. Means ± standard deviations were obtained from three independent series of experiments.

Cells Accumulate at G2/M Phase in Relation to Partial Gravity Exposure

As simulated microgravity slows down the cell cycle progression of myoblasts (Benavides Damm et al., 2013a), we hypothesized that the decelerated proliferation rate observed in myoblasts grown under partial gravity is also due to retardation in the cell cycle. As the Two Velocities algorithm showed the most consistent relation between the level of simulated gravity exposure and proliferation, only this algorithm was tested for cell cycle analysis. In this case, the percentage of cells in G0/G1 and S phases increased (Fig. 6A) while the percentage in G2/M phase decreased (Fig. 6B) as the partial gravity values augmented. Specifically, the percentage of cells accumulated within the G2/M phase were $38.95 \pm 6.54\%$ at 0 g, $31.68 \pm 4.97\%$ at 0.2 g, $26.95 \pm 4.87\%$ at 0.4 g, $21.55 \pm 3.33\%$ at 0.6 g, and $16.40 \pm 1.98\%$ in the 1 g control. By fitting the data into a linear regression model (Fig. 6C), a correlation value equal to 0.98 was obtained, indicating the close relation between G2/M phase accumulation and the simulated partial gravity level. It is remarkable that the same effect observed in cell proliferation is also detected in the cell cycle analysis, where the magnitude of the effect depends on the extent of partial gravity exposure. As we have previously shown, the slowed proliferation observed in the mouse myoblasts might thus be explained by a delay in the G2/M phase progression after 10 h of cultivation on the RPM (Benavides Damm et al., 2013b). To discard the possibility that the particular protocol followed when performing experiments on the RPI causing false positive results, two control experiments were conducted at the same time with cells cultured at 1 g. Therefore, additional samples were placed inside a standard laboratory CO_2 incubator filled with culture media (Ctrl) and under normal culture conditions (Inc). The analysis showed no difference between these two controls, indicating that our experimental protocol does not lead to an artifact on the RPI

samples. Subsequently, the effects we observed are caused merely by simulated partial gravity exposure.

Lymphocyte Activation Rate is Dependent on the Level of Partial Gravity Exposure

It has been known for decades that the activation of lymphocytes is severely impaired under microgravity conditions in space (Bechler et al., 1992; Cogoli et al., 1984). We therefore investigated a potential relation between the different levels of simulated gravity ranging from 0.2 to 0.6 g (by using the three algorithms introduced) and the activation rate of lymphocytes. Cells activated in the presence of simulated 0.2 g using the Two Velocities algorithm were as poorly activated as the 0 g samples, whereas the cells activated at simulated 0.6 g responded similarly to the 1 g control, standardized as 100% of activation (Fig. 7). Interestingly, the activation level of the 0.4 g exposed cells was almost in the middle of the two other gravity levels (0.2 and 0.6 g). Although the level of gravity was correlated with the level of lymphocyte activation in all three simulation modes, the effect of simulated partial gravity using the Two Velocities algorithm led to an analogous correlation pattern compared to the results gathered with the C2C12 cells. With this algorithm, the percentage of activated cells went from $39.29 \pm 6.32\%$ at 0.2 g, to $68.20 \pm 23.09\%$ at 0.4 g, and $80.60 \pm 21.29\%$ at 0.6 g.

Discussion

Our upgraded RPI offers the possibility of studying cellular systems during simulated microgravity as well as partial gravity environments, an advantage over previous microgravity simulating devices like the classical RPM where a variety of gravity levels was not possible. Mounting the incubator on the rotating frame instead of placing a small RPM into an incubator brings several advantages not yet
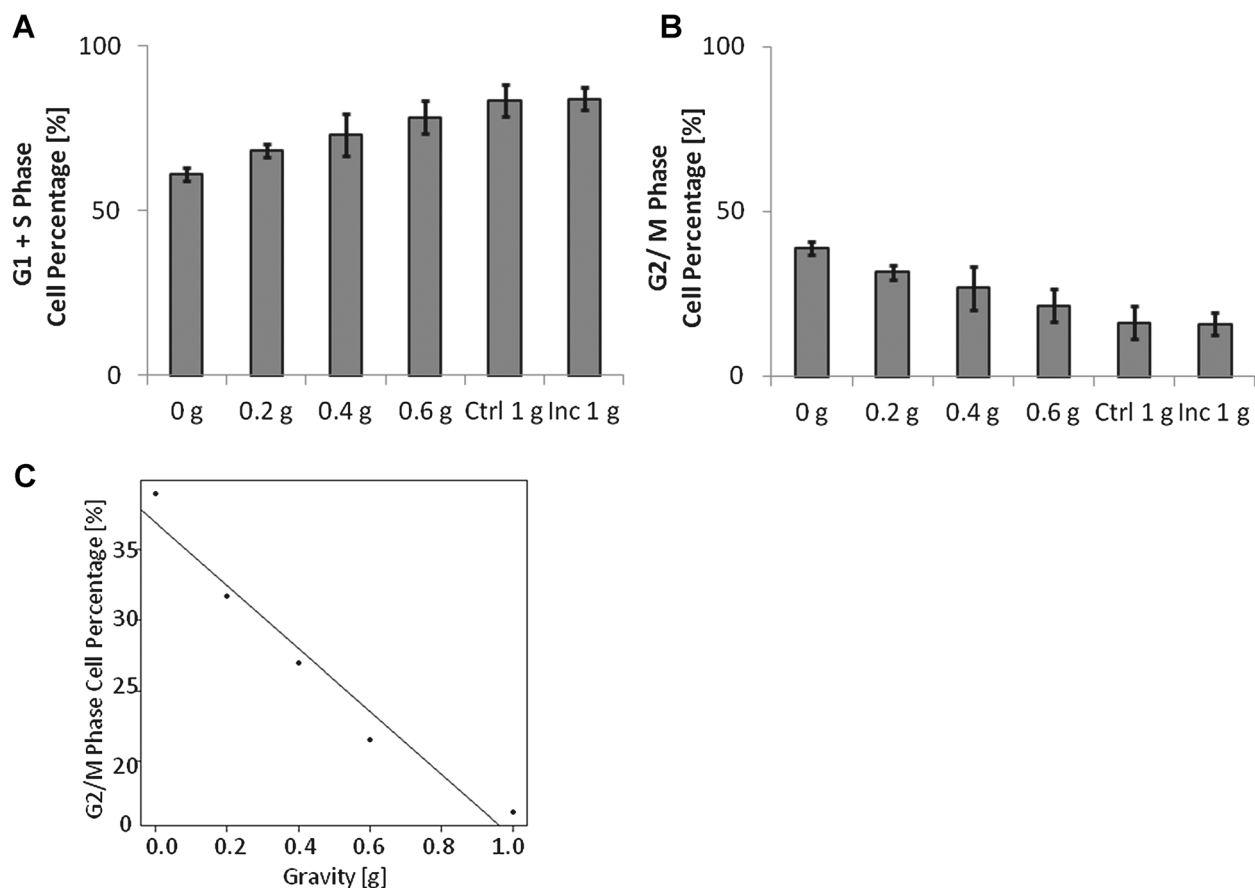
Figure 6. Partial gravity causes cells to accumulate at G2/M phase. Cells were collected 10 h after cultivation under partial gravity (RPI) or at 1 g (Ctrl and Inc). The Two Velocities algorithm was used to obtain partial gravity (see Materials and Methods). The cell cycle was analyzed and the percentage of cells in G0/G1 + S phase (**A**) and in the G2/M phase (**B**) is displayed, as well as the linear regression model with data from G2/M phase cell percentages (**C**). Means ± standard deviations were obtained from four independent series of experiments.
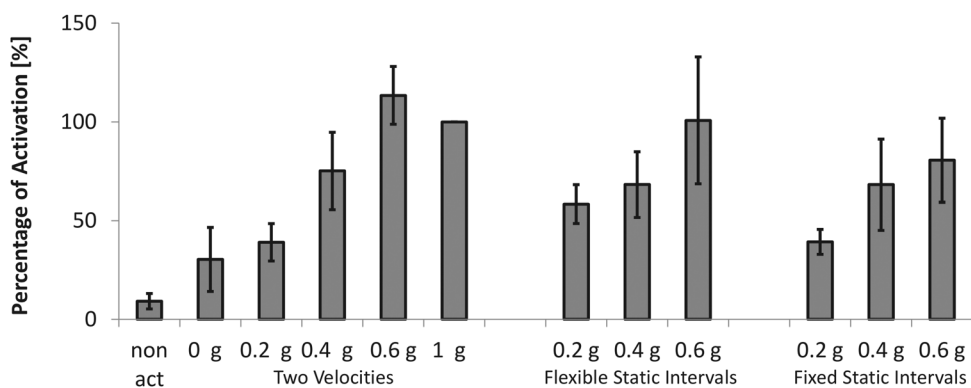

Figure 7. Lymphocyte activation depends on partial gravity exposure. Cells were treated after an adaptation period of 60 to 90 min with an activator solution and then cultured for 20 to 22 h on the RPI. Three different algorithms for partial gravity simulation (see Materials and Methods) were compared in the following order: Two Velocities, Flexible Static Intervals, and Fixed Static Intervals. The 1 g samples of each experiment were considered as 100% activated, and were used to standardize the other samples among the different experiments. A non-activated sample was used as a negative control. Means ± standard deviations were obtained from three independent series of experiments.

found with other products, such as: the volume available for tests is larger, offering therefore more samples to be tested under identical conditions at the same time; the sample contamination originating from the machinery is completely avoided (e.g., through outgassing/offgassing from oil-grease lubrication, from the electronic circuitry and its cabling, and from wear debris); the test conditions can be controlled much better as the essential parameters (like temperature, CO_2 levels, etc.) are more homogeneously distributed because there is no heat dissipation and unplanned ventilation by a rotating motorized equipment in the incubator; the addition of supplementary functions, such as daylight and UV illumination, do not interfere with the machinery exigencies installed in the incubator.

By illustrating the behavior of cells at different gravitational loads, our RPI helps to unravel how partial gravity affects the biological processes necessary to sustain life in different space scenarios, such as on the Moon or Mars. Furthermore, this knowledge facilitates the comprehension of the mechanobiological processes that happen within each cell on earth, from sensing the diverse gravitational forces to transducing the signals through various pathways to elicit an appropriate response. Defects in mechanotransduction may appear as deficits in cellular structure and organization, impairing mechanosensation, or as mutations or deregulations in the proteins involved in the downstream signaling pathways, directly affecting the normal mechanoresponse. In order to improve our understanding of such faulty responses and consequently develop efficient therapeutic strategies against the related diseases it is important to identify the molecular components encompassing normal and defective mechanotransduction. The omnipresent gravitational force can be regarded as a physical force influencing cells, tissues, and organs as other forces do, gravity thus exerts a mode of mechanical input to cells that can have profound biological implications. Studying the behavior of cells cultured under different gravitational loads broadens our understanding of disorders related to mechanical stimulation relevant not only for astronauts exposed to low gravity, but also for patients on earth suffering for example from muscle wasting disorders or a weak immune system. Our experimental data obtained here from two different cell types (mouse skeletal myoblasts and human lymphocytes) demonstrated their sensitivity to the gravitational environment by proving a strong correlation between the different levels of simulated gravity exposure and the observed biological effect in a reproducible manner.

Three different algorithms for simulating partial gravity were tested and the cellular response was compared. On the one hand, the mouse myoblasts showed a reduction in the proliferation rate, while cells accumulated in the G2/M phase of the cell cycle in parallel with decreasing values of simulated gravity (Figs. 4 and 6). On the other hand, the activation rate of human lymphocytes dropped with a decline in gravity level (Fig. 7). In addition, data obtained from the lymphocyte experiment demonstrated a strong correlation between the level of activation and the magnitude of the simulated gravity field regardless of the type of algorithm applied. In contrast, a relation between the proliferation rate and the gravity level in the myoblasts was observed only when using the Two Velocities and the Flexible Static Intervals algorithms. Perhaps the Fixed Static Intervals algorithm triggers an effect in these cells that seems to be threshold dependent, where the cells respond only after reaching this threshold, regardless of the actual gravity value that is simulated by the RPI. The different reactions of the two types of cells (myoblasts and lymphocytes) might be due to the fact that they are adherent and free floating cells, respectively. Therefore, in the Fixed Static Intervals algorithm, the fixed time in static position might be more easily recognized by adherent cells than by free floating cells. In this case, it could be that the time the myoblasts spent at 1 g was already long enough to trigger the normal terrestrial response in a percentage of the cells, whereas the time spent at 0 g could trigger the opposite effect on the remaining percentage of cells, averaging as a result of a time duration threshold.

Calcium signals control various cellular responses in skeletal muscle as well as in lymphocytes (Bassel-Duby and Olson, 2006; Clapham, 2007; Lewis, 2001). Indeed, we previously described how disturbed calcium entry through mechanosensitive channels affects proliferation, cell cycle progression, and gene expression during simulated microgravity (Benavides Damm et al., 2013b). The difference in cellular responses between the three algorithms tested for partial gravity could therefore be caused by diversions in calcium entry which impinge on downstream signaling pathways. Thus on the one hand, the cells would sense the partial gravity level at which they are exposed through calcium channels, and depending on the algorithm, this could be enough to elicit a linear response according to the gravitational force where cells respond gradually to the mechanical unloading. On the other hand, the stimulation could trigger an effect on calcium entry only when a certain threshold is reached, impounding the expected cellular response.

Though difficult to correlate with our results from single cell behavior, studies performed on whole organisms have shown a similar trend when measuring various parameters in different partial gravity environments. During parabolic flights, human subjects showed that the external work required to walk a given distance is significantly less at lower gravity (Cavagna et al., 2000). Consistently, a study done on suspended subjects with a strapped harness reported that the vertical, forward, and total external work per stride also declined following a linear trend with diminishing gravity (Griffin et al., 1999). In a similar study performed on suspended mice, the peak hind limb force was reduced as well linearly with decreasing gravity values (Wagner et al., 2010). As for experiments performed on humans underwater with a treadmill and an adjustable ballasting harness, the results are in agreement with the data mentioned above (Newman and Alexander, 1993). Research focusing on load-carrying in partial gravity also by underwater immersion confirmed that energy expenditure and stride rates dropped while the forward lean exhibited by subjects increased dramatically with diminishing gravity levels (Wickman and Luna, 1996).

Recently, the possibility of humans running in place on water was investigated, where the subjects, suspended with a harness, experienced different levels of partial gravity just above the water. The predicted available impulse and the number of successful subjects that could generate enough muscle power to run in place over a wading pool decreased linearly with increasing gravity levels (Minetti et al., 2012). Other studies performed on humans, also under suspension, have focused on the performance of chest compressions under partial and microgravity. In both reports, the mean frequency of external chest compression did not result in a pattern relative to the level of gravity exposure in either male or female subjects (Dalmarco et al., 2006; Kordi et al., 2012). On another area of research, investigators studied the human perception of verticality during a recent parabolic flight campaign of partial gravity. In this case, the authors found out that the gravity level must exceed a certain threshold to be recognized as a reference for verticality, which was of 0.3 g, depicting an onset where the effect of gravity exposure was detected (de Winkel et al., 2012).

In summary, there are three different outcomes that can be detected with changing partial gravity values: a linear effect, a result that depends on a certain threshold, and no correlation between the exposure level and the response. As whole organisms respond differently than single cells, an explanation for what we observe cannot be attained from the studies mentioned above. For that reason, our new RPI uniquely provides the advantage of studying single cell behavior, something that was not possible until now. In this way, our RPI mediates a valuable tool to perform cell experiments under partial gravity environments where the exact mechanoresponse that gives rise to specific signals in each individual cell can be investigated as a reaction from mechanical unloading.

Conclusions

We are introducing a novel instrument called RPI for 3D cell culturing that in addition to growing cells under simulated microgravity, allows the generation of a partial earth-like gravity field of various values. Therefore, studies of cell growth behavior under a nullified gravity vector environment as well as under different simulated gravity fields (from 0 to 1 g) are now possible. Such a technique opens new aspects of biotechnology and enables the study of fundamental cellular mechanisms modulating mechanically-regulated tissue development and maintenance.

In our frame of study there appears to be two different responses to changes in partial gravity, one being set by a threshold from where the effect can be detected, and the other one varying in proportion to the gravity exposure level. In this report, we have unraveled the possibility of exploring the effects of partial gravity on biological samples at an earth-bound facility in a comparable manner. To our knowledge, this is the first time simulated partial gravity has been achieved by using a RPM-like device. The techniques that

have been used so far to simulate partial gravity include ballasted underwater immersion, parabolic flights, over-head suspension, off-loading pulley systems, and tilted bed rest studies (Louisy et al., 1994; Newman, 2000). However, all of these have specific advantages and disadvantages. On the one hand, the over-head suspension, off-loading pulley systems, and tilted bed rest studies are economical techniques, but they are not suitable for cell culture analyses and they restrict the freedom of movement in humans and animals. While underwater immersion has no constraints on movement, it entails an inconvenient hydrodynamic drag. On the other hand, parabolic flights offer freedom of movement, with no hydrodynamic drag, and are appropriate for cell culture studies, but they are expensive and the partial gravity exposure only lasts for a short duration (ranging approximately from 20 to 40 s). Moreover, on-board centrifuge facilities inside a spacecraft have been suggested to enable investigators to study the effects of partial gravity (Wagner and Fulford-Jones, 2006). This comes, however, at an expensive cost and is limited to a few experiments only, restricting the amount of data that can be gathered. For these reasons, our newly designed and built RPI is a breakthrough tool that will enable scientists to investigate partial gravity on cell cultures and small organisms for up to a long duration at the gravity field of interest, such as that of the Moon or Mars, with countless reproducible experiments and at an economic cost. In addition to broadening the scope of available tools to study the behavior of biological systems affected by space travel, our RPI can be employed as a method to explore the effects of mechanical unloading on cells through partial gravity, being a relevant model system with which to better understand the cellular responses subsequent to mechanotransduction. Studying the underlying mechanisms that regulate muscle development and the immune system activation under partial gravity exposure is crucial for the identification of the causes and countermeasures for trauma and earth-bound diseases as well as to improve the sustainment of human life in space.

References

Baharvand H, Hashemi SM, Kazemi Ashtiani S, Farrokhi A. 2006. Differentiation of human embryonic stem cells into hepatocytes in 2D and 3D culture systems in vitro. Int J Dev Biol 50(7):645–652.

Bassel-Duby R, Olson EN. 2006. Signaling pathways in skeletal muscle remodeling. Annu Rev Biochem 75:19–37.

Bechler B, Cogoli A, Cogoli-Greuter M, Muller O, Hunzinger E, Criswell SB. 1992. Activation of microcarrier-attached lymphocytes in microgravity. Biotechnol Bioeng 40(8):991–996.

Benavides Damm T, Franco-Obregon A, Egli M. 2013a. Gravitational force modulates G 2/M phase exit in mechanically unloaded myoblasts. Cell Cycle 12(18):3001–3012.

Benavides Damm T, Richard S, Tanner S, Wyss F, Egli M, Franco-Obregon A. 2013b. Calcium-dependent deceleration of the cell cycle in muscle cells by simulated microgravity. FASEB J 27(5):2045–2054.

Block I, Briegleb W, Wohlfarth-Bottermann KE. 1986. Gravisensitivity of the acellular slime mold Physarum polycephalum demonstrated on the fast-rotating clinostat. Eur J Cell Biol 41:44–50.

Cavagna GA, Willems PA, Heglund NC. 2000. The role of gravity in human walking: Pendular energy exchange, external work and optimal speed. J Physiol 528(Pt 3):657–668.

Chang TT, Walther I, Li CF, Boonyaratanakornkit J, Galleri G, Meloni MA, Pippia P, Cogoli A, Hughes-Fulford M. 2012. The Rel/NF-kappaB pathway and transcription of immediate early genes in T cell activation are inhibited by microgravity. J Leukoc Biol 92(6):1133–1145.

Clapham DE. 2007. Calcium signaling. Cell 131(6):1047–1058.

Cogoli A, Tschopp A, Fuchs-Bislin P. 1984. Cell sensitivity to gravity. Science 225(4658):228–230.

Dalmarco G, Calder A, Falcao F, de Azevedo DF, Sarkar S, Evetts S, Moniz S, Russomano T. 2006. Evaluation of external cardiac massage performance during hypogravity simulation. Conf Proc IEEE Eng Med Biol Soc 1:2904–2907.

de Winkel KN, Clement G, Groen EL, Werkhoven PJ. 2012. The perception of verticality in lunar and Martian gravity conditions. Neurosci Lett 529(1):7–11.

Freed LE, Vunjak-Novakovic G. 1995. Cultivation of cell-polymer tissue constructs in simulated microgravity. Biotechnol Bioeng 46(4):306–313.

Friedrich UL, Joop O, Putz C, Willich G. 1996. The slow rotating centrifuge microscope NIZEMI–a versatile instrument for terrestrial hypergravity and space microgravity research in biology and materials science. J Biotechnol 47(2–3):225–238.

Griffin TM, Tolani NA, Kram R. 1999. Walking in simulated reduced gravity: Mechanical energy fluctuations and exchange. J Appl Physiol 86(1):383–390.

Herranz R, Benguria A, Laván DA, López-Vidriero I, Gasset G, Javier Medina F, Van L, Jwa J, Marco R. 2010. Spaceflight-related suboptimal conditions can accentuate the altered gravity response of Drosophila transcriptome. Mol Ecol 19(19):4255–4264.

Hoson T, Kamisaka S, Masuda Y, Yamashita M, Buchen B. 1997. Evaluation of the three-dimensional clinostat as a simulator of weightlessness. Planta 203(Suppl):S187–S197.

Infanger M, Kossmehl P, Shakibaei M, Bauer J, Kossmehl-Zorn S, Cogoli A, Curcio F, Oksche A, Wehland M, Kreutz R, Paul M, Grimm D. 2006. Simulated weightlessness changes the cytoskeleton and extracellular matrix proteins in papillary thyroid carcinoma cells. Cell Tissue Res 324(2):267–277.

Kordi M, Kluge N, Kloeckner M, Russomano T. 2012. Gender influence on the performance of chest compressions in simulated hypogravity and microgravity. Aviat Space Environ Med 83(7):643–648.

Lewis RS. 2001. Calcium signaling mechanisms in T lymphocytes. Annu Rev Immunol 19:497–521.

Louisy F, Guezennec CY, Guell A. 1994. Leg vein hemodynamics during bedrests simulating lunar trip. J Gravit Physiol 1(1):P100–P101.

Minetti AE, Ivanenko YP, Cappellini G, Dominici N, Lacquaniti F. 2012. Humans running in place on water at simulated reduced gravity. PLoS ONE 7(7):e37300.

Newman DJ. 2000. Life in extreme environments: How will humans perform on Mars? Gravit Space Biol Bull 13(2):35–47.

Newman DJ, Alexander HL. 1993. Human locomotion and workload for simulated lunar and Martian environments. Acta Astronaut 29(8):613–620.

Pavy-Le Traon A, Allevard AM, Fortrat JO, Vasseur P, Gauquelin G, Guell A, Bes A, Gharib C. 1997. Cardiovascular and hormonal changes induced by a simulation of a lunar mission. Aviat Space Environ Med 68(9):829–837.

Pietsch J, Sickmann A, Weber G, Bauer J, Egli M, Wildgruber R, Infanger M, Grimm D. 2012. Metabolic enzyme diversity in different human thyroid cell lines and their sensitivity to gravitational forces. Proteomics 12(15–16):2539–2546.

Rivera-Solorio I, Kleis SJ. 2006. Model of the mass transport to the surface of animal cells cultured in a rotating bioreactor operated in micro gravity. Biotechnol Bioeng 94(3):495–504.

Saltzman WM, Parkhurst MR, Parsons-Wingerter P, Zhu WH. 1992. Three-dimensional cell cultures mimic tissues. Ann NY Acad Sci 665:259–273.

Schwarz RP, Goodwin TJ, Wolf DA. 1992. Cell culture for three-dimensional modeling in rotating-wall vessels: An application of simulated microgravity. J Tissue Cult Methods 14(2):51–57.

Schwarzenberg M, Pippia P, Meloni MA, Cossu G, Cogoli-Greuter M, Cogoli A. 1999. Signal transduction in T lymphocytes—A comparison of the data from space, the free fall machine and the random positioning machine. Adv Space Res 24(6):793–800.

Sonnenfeld G. 2012. Editorial: Space flight modifies T cellactivation-role of microgravity. J Leukoc Biol 92(6):1125–1126.

Sun T, Jackson S, Haycock JW, MacNeil S. 2006. Culture of skin cells in 3D rather than 2D improves their ability to survive exposure to cytotoxic agents. J Biotechnol 122(3):372–381.

van Loon JJWA. 2007. Some history and use of the random positioning machine, RPM, in gravity related research. Adv Space Res 39(7):1161–1165.

Vandenburgh H, Chromiak J, Shansky J, Del Tatto M, Lemaire J. 1999. Space travel directly induces skeletal muscle atrophy. FASEB J 13(9):1031–1038.

Wagner EB, Fulford-Jones TR. 2006. Sensorimotor investigations for the Mars Gravity Biosatellite: A rotating spacecraft for partial gravity research. Brain Res 1091(1):75–78.

Wagner EB, Granzella NP, Saito H, Newman DJ, Young LR, Bouxsein ML. 2010. Partial weight suspension: A novel murine model for investigating adaptation to reduced musculoskeletal loading. J Appl Physiol 109(2):350–357.

Watson JV, Chambers SH, Smith PJ. 1987. A pragmatic approach to the analysis of DNA histograms with a definable G1 peak. Cytometry 8(1):1–8.

Wickman LA, Luna B. 1996. Locomotion while load-carrying in reduced gravities. Aviat Space Environ Med 67(10):940–946.

Yip DK, Auersperg N. 1972. The dye-exclusion test for cell viability: Persistence of differential staining following fixation. In Vitro 7(5):323–329.